Available online at www.sciencedirect.com
SCIENCE DIRECT®
Journal of Sound and Vibration 285 (2005) 51–71
JOURNAL OF SOUND AND VIBRATION
www.elsevier.com/locate/jsvi

Oscillations of captured spherical drop of viscous liquid

H.F. Bauer[a], M. Chiba[b,*]

[a]*Institut für Raumfahrttechnik, Universität der Bundeswehr München, 85577 Neubiberg, Germany*
[b]*Department of Mechanical Engineering, Faculty of Engineering, Iwate University, 4-3-5 Ueda, Morioka 020-8551, Japan*

Received 2 February 2004; received in revised form 15 June 2004; accepted 11 August 2004
Available online 15 December 2004

Abstract

The complex frequencies of a viscous spherical drop where part of the free surface is embedded in a rigid spherical cap of the same radius have been determined as a function of the cap angle and the free surface tension parameter. With increasing cap angle α, the oscillation frequencies and decay magnitudes increase. This is also true for liquid drops of larger surface tension parameters. It also could be found, as has been found previously for a free floating sphere of viscous liquid, that the oscillations may cease to exist for certain diameters and low surface tension parameters, a fact not present in the treatment of frictionless liquid. In such cases, the captured liquid globule performs just an aperiodic motion. Three different liquid systems have been considered. In addition, the response of a captured spherical drop due to harmonically forced vertical translational excitation of the cap has been determined. Only a liquid sphere embedded in a spherical cap of the same radius has been evaluated numerically. The results reveal that for the mode $n = 1$ the geometry of a liquid sphere in a spherical cap of equal radius represents—depending on the magnitude α of the cap—for small surface tension parameters $\sigma^* \equiv \sigma a\rho/\eta^2$, a stable configuration, while for large σ^*-values the spherical geometry is unstable, indicating that for those large cases the free liquid surface assumes a different geometry.

*Corresponding author. Tel.:/fax: +81 19 621 6404.
E-mail address: mchiba@iwate-u.ac.jp (M. Chiba).

0022-460X/$ - see front matter © 2004 Elsevier Ltd. All rights reserved.
doi:10.1016/j.jsv.2004.08.004

Nomenclature

$\bar{A}_n \sim \bar{D}_n$	coefficients of Eq. (9)
$A_n \sim D_n$	coefficients of Eqs. (10) and (11), $A_n \equiv \bar{A}_n/a^2$
a	radius of drop
b	radius of core or center sphere
$\bar{E}_n, \bar{F}_n$	coefficients of Eq. (8)
$\mathrm{I}_n, \mathrm{K}_n$	modified Bessel functions
i	imaginary unit
k	radius ratio for annular drop $\equiv b/a$
m	angular mode number
Oh	Ohnesorge-number
p	pressure
$\tilde{R}e_\sigma$	capillary Reynolds-number
r, ϑ, φ	coordinate system
s	complex frequency $(= \bar{\sigma} + \mathrm{i}\bar{\omega})$, $S = sa^2/\nu$
t	time
$P_n^m(\cos\vartheta)$	associated Legendre function
u, υ, w	velocity components of drop $(\vec{v} = u\vec{e}_r + \upsilon\vec{e}_\vartheta + w\vec{e}_\varphi)$ in radial-, meridional- and angular direction, respectively
V_0	drop volume
x, y, z	coordinate system
Z_0	amplitude of excitation force in z direction $(\bar{Z}_0 \equiv Z_0\nu/a^2)$
α	cap area of drop: $0 < \alpha < \pi$ $(\bar{\alpha} = \alpha/\pi)$
ζ	free surface displacement from equilibrium position $r = a$
η	dynamic viscosity
ν	kinematic viscosity $(= \eta/\rho)$
ρ	density of drop
σ	surface tension $(\sigma^* \equiv \sigma a/\rho\nu^2 = (\tilde{R}e_\sigma)^2 = (Oh)^{-2})$
$\tau_{r\vartheta}, \tau_{r\varphi}$	shear stresses
ψ	stream function
Ω	circular forcing frequency $(\Omega^* = \mathrm{i}\Omega a^2/\nu)$

1. Introduction

The drastically reduced gravity force in a microgravity environment makes surface tension the major force influencing the motion of liquids. As the force of gravity approaches zero, the equilibrium position of a liquid drop assumes a perfect spherical geometry. The behavior of a freely floating or captured liquid system finds application not only in mechanical sciences and metallurgy but also in chemical engineering, nuclear fission as well as in geological and astrophysical engineering. In recent years, fluid dynamics problems concerning the sphere and the so-called liquid bridge, i.e. cylindrical liquid column attached to a top- and bottom disc of the same diameter as the liquid column have been subject to intense investigations in zero gravity. The liquid in such studies was always considered incompressible and was either frictionless, viscous or visco-elastic. In addition, some investigations treated spinning columns that rotated about the longitudinal axis in order to find a reduced wave pattern on the cylindrical free liquid surface.

A viscous drop partially embedded in a spherical cap has not been treated and attracts already by its sheer existence some intellectual curiosity. A captured liquid drop is described here by a spherical globule where part of the free surface is embedded in a rigid spherical part of the same radius. The dynamical behavior of such a system is important to solidification processes of a molten material or just to a liquid drop, of which part of the free liquid surface is replaced by a solid spherical cap. The paper treats the vibrational behavior of a liquid globule in partial contact with a spherical cap. It investigates the prerequisites for some prospects that will be offered by future Spacelab- and Space station-Missions, where the growing and possibly manufacturing of crystals of high pureness and homogeneity in a zero- or micro-gravity environment may be

attempted. Such crystal growth experiments have previously already been performed for cylindrical configurations, i.e. liquid bridges in some Skylab and Spacelab flights and seem to promise a successful manufacturing procedure for mono-crystals. To grow and produce, however, pure crystals of high quality, it is necessary to investigate the vibrational behavior and its detrimental effects on a growing crystal and estimate a more favorable vibrational environment for the growth procedure, that has to be observed for proper manufacturing. The embedded liquid sphere exhibits, due to the reduced free surface area of the liquid, increased natural frequencies as well as drastically changed mode shapes.

A remarkable series of experiments on these and related problems have been performed by Plateau [1] in the years from 1843 to 1869. In 1879, Lord Rayleigh [2,3] investigated the vibrations of a liquid mass of spherical configuration and determined the natural frequencies of modes being symmetric to an axis of the sphere. Later Lamb [4] gave a slightly generalized result by assuming that the sphere with density ρ_2 is surrounded by an infinite liquid medium of density ρ_1. For a small viscosity of the liquid, Lamb [5] presented its influence upon the frequency of oscillations. Immersed freely floating viscous drops have been treated in Refs. [6,7]. A large variety of spherical configurations has been treated for frictionless liquid by Bauer [8]. The natural frequencies and stability of some basic spherical liquid systems have also been presented for inviscid and viscous liquids in Ref. [9], in which in addition to Ref. [10] a few cases of immiscible spherical liquid arrangement have been considered.

But in addition, results for nonlinear motion of capillary surface waves have been presented in Refs. [11,12] and in 1973 a numerical treatment of the problem has been performed [13] for large amplitude vibrations. Some investigations have also been performed for freely floating liquid spheres consisting of visco-elastic material [14–16]. Including viscosity in the treatment shows that some configurations, i.e., the magnitude of the liquid surface tension parameter $\sigma^* \equiv \sigma a/\rho v^2$ and the magnitude of the diameter $2a$ of the liquid sphere yield only aperiodic motion for the liquid system. For liquid spheres partly captured and embedded in a rigid spherical cap exhibiting the same radius as the drop, the oscillatory behavior of an inviscid liquid has been investigated for various configurations in Ref. [17]. It was found that with increasing cap angle α the natural frequencies increase, exhibiting also larger increases for higher modes. In addition the mode shapes are drastically changed. A new mode shape in the presence of a cap was detected. It is the mode corresponding to the mode shape of zero frequency in a freely floating drop, where the motion describes the rigid body motion of the sphere without change of the free surface area of the drop. For a liquid sphere embedded in a spherical cap, this mode $n = 1$ definitely exhibits during oscillation a change of the free surface area. In addition, the response of the captured sphere due to harmonically forced translational excitation of the cap in two major directions has been investigated in that paper [17].

The behavior of a viscous liquid sphere in partial contact with a solid spherical cap of the same radius has not been studied yet. Therefore the following paper investigates the oscillatory- and decay behavior of a viscous and partly embedded liquid sphere in a cap of the same radius under zero-gravity condition. The complex natural frequencies are determined as a function of the magnitude of the rigid cap angle α and the free surface tension σ^*, where σ^* could also be considered as the square of the capillary Reynolds number $\sigma^* = (\tilde{R}e_\sigma)^2$ or as the often used Ohnesorge number $\sigma^* = (Oh)^{-2}$. The results are compared with the results of the frictionless case as well as with the freely floating viscous sphere ($\alpha = 0$).

2. Basic equations

A spherical drop of volume $V_0 = \frac{4\pi}{3}a^3$ or an annular drop of volume $V_0 = \frac{4\pi}{3}a^3(1-k^3)(k = b/a)$ is in a zero-gravity environment and is partly captured by a spherical wall of the same radius a, covering a certain given range in the meridian coordinate ϑ (Fig. 1). If subjected to a disturbance, the captured liquid globule will perform damped oscillations. The following shall investigate axisymmetric oscillations of such systems for a viscous liquid. No assumption is made with respect to the contact angle, i.e., whether the liquid is hydrophilic (wetting) or hydrophobic (non-wetting). We assume that the liquid is anchored at the rim of the cap.

If the liquid is incompressible and viscous, exhibiting the density ρ and performing oscillations with small free surface displacements $\zeta\,(|\zeta/a| \ll 1)$ and small velocities, the motion of such a captured liquid globule system is described by the Stokes equation

$$\frac{\partial \vec{v}}{\partial t} + \frac{1}{\rho}\operatorname{grad} p + \nu \operatorname{curl}\operatorname{curl}\vec{v} = 0 \tag{1}$$

and the continuity equation

$$\operatorname{div}\vec{v} = 0. \tag{2}$$

These equations have to be solved with the appropriate boundary conditions of vanishing velocities (adhesive conditions) at the spherical walls, and vanishing shear stress $\tau_{r\vartheta} = \tau_{r\varphi} = 0$ at the free surface ranges, as well as the combined free surface condition

$$\frac{\partial p}{\partial t} - 2\eta\frac{\partial^2 u}{\partial r \partial t} + \frac{\sigma}{a^2}\left\{2u + \frac{1}{\sin\vartheta}\frac{\partial}{\partial\vartheta}\left(\sin\vartheta\frac{\partial u}{\partial\vartheta}\right) + \frac{1}{\sin^2\vartheta}\frac{\partial^2 u}{\partial\varphi^2}\right\} = 0, \tag{3}$$

at the ranges of the free liquid surface areas. The solutions of these equations constitute the free oscillation problem of a given captured liquid globule system. They will reveal the damped natural frequencies of the oscillation modes as a function of the size of the rigid cap (in which the liquid globule is embedded) and shall present the course of these complex frequencies with the increase of the surface tension parameter or capillary Reynolds number.

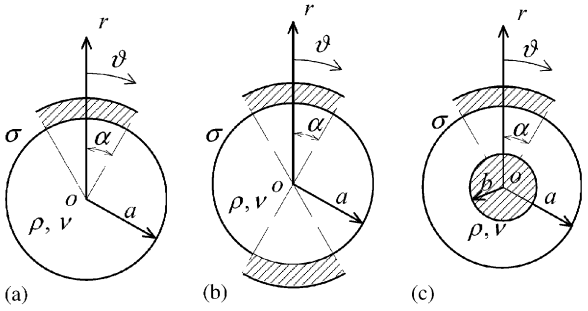

Fig. 1. Captured spherical viscous drop system: (a) simple liquid sphere; (b) spherical drop captured at both poles; (c) annular spherical liquid system.

In addition, the goal is a closer investigation of the newly appearing fundamental mode, which is in a freely floating liquid sphere represented with the frequency zero, i.e., a rigid body motion without change of the free surface, expressing a vanishing capillary restoring force. Depending on the magnitude of the surface tension parameter and the cap angle, the liquid may not oscillate at all, but perform just an aperiodic motion if disturbed.

3. Method of solution

In the following, we shall investigate first the damped natural frequencies (complex frequencies) of captured viscous liquid drops. The geometry and coordinate system used are presented in Fig. 1. The results are based on axisymmetric motion of the system ($\partial/\partial\varphi \equiv 0, w \equiv 0$) and shall yield the approximate lower damped natural frequencies for systems of various magnitudes of α.

For axisymmetric motion ($\partial/\partial\varphi \equiv 0, w \equiv 0$), we introduce the stream function $\psi(r, \vartheta, t)$, such that the continuity equation (2) is satisfied identically, i.e.,

$$u = -\frac{1}{r^2 \sin\vartheta}\frac{\partial\psi}{\partial\vartheta} \quad \text{and} \quad v = \frac{1}{r \sin\vartheta}\frac{\partial\psi}{\partial r} \tag{4}$$

and obtain, after eliminating the pressure p, the partial differential equation of the stream function

$$\bar{\Delta}\left[\bar{\Delta}\psi - \frac{1}{\nu}\frac{\partial\psi}{\partial t}\right] = 0, \tag{5}$$

where the operator is

$$\bar{\Delta} \equiv \frac{\partial^2}{\partial r^2} + \frac{\sin\vartheta}{r^2}\frac{\partial}{\partial\vartheta}\left(\frac{1}{\sin\vartheta}\frac{\partial}{\partial\vartheta}\right). \tag{6}$$

Applying the vector operation "divergence" to the Stokes equation (1) yields the Laplace equation for the pressure

$$\Delta p = 0, \tag{7}$$

which exhibits the solution

$$p(r, \vartheta, t) = \sum_{n=1}^{\infty}\left[\bar{E}_n\left(\frac{r}{a}\right)^n + \bar{F}_n\left(\frac{r}{a}\right)^{-(n+1)}\right] P_n^0(\cos\vartheta)\mathrm{e}^{st} + \frac{2\sigma}{a}, \tag{8}$$

where $s = \bar{\sigma} + \mathrm{i}\bar{\omega}$ represents the complex frequency which has to be determined. The solution of Eq. (5) is given by

$$\psi(r, \vartheta, t) = \sum_{n=1}^{\infty}\left\{\bar{A}_n\left(\frac{r}{a}\right)^{n+1} + \bar{B}_n\left(\frac{r}{a}\right)^{-n} + \bar{C}_n\left(\frac{r}{a}\right)^{1/2}\mathrm{I}_{n+1/2}\left(\sqrt{S}\frac{r}{a}\right) + \bar{D}_n\left(\frac{r}{a}\right)^{1/2}\mathrm{K}_{n+1/2}\left(\sqrt{S}\frac{r}{a}\right)\right\} \times \sin\vartheta P_n^1(\cos\vartheta)\mathrm{e}^{st}, \tag{9}$$

where $S \equiv sa^2/\nu$ and $\mathrm{I}_{n+1/2}$ and $\mathrm{K}_{n+1/2}$ are modified Bessel functions and $P_n^0(\cos\vartheta)$ and $P_n^1(\cos\vartheta)$ are the associated Legendre functions. The velocity distribution is given by

$$u(r,\vartheta,t) = \sum_{n=1}^{\infty}\left\{A_n\left(\frac{r}{a}\right)^{n-1} + B_n\left(\frac{r}{a}\right)^{-(n+2)} + C_n\left(\frac{r}{a}\right)^{-3/2}\mathrm{I}_{n+1/2}\left(\sqrt{S}\frac{r}{a}\right) + D_n\left(\frac{r}{a}\right)^{-3/2}\mathrm{K}_{n+1/2}\left(\sqrt{S}\frac{r}{a}\right)\right\} \times n(n+1)P_n^0(\cos\vartheta)\mathrm{e}^{st} \tag{10}$$

and

$$\upsilon(r,\vartheta,t) = \sum_{n=1}^{\infty}\left\{A_n(n+1)\left(\frac{r}{a}\right)^{n-1} - B_n n\left(\frac{r}{a}\right)^{-(n+2)} + C_n\left[\frac{r}{a}\sqrt{S}\mathrm{I}_{n-1/2}\left(\sqrt{S}\frac{r}{a}\right) - n\mathrm{I}_{n+1/2}\left(\sqrt{S}\frac{r}{a}\right)\right] \times\left(\frac{r}{a}\right)^{-3/2} - D_n\left[\frac{r}{a}\sqrt{S}\mathrm{K}_{n-1/2}\left(\sqrt{S}\frac{r}{a}\right) + n\mathrm{K}_{n+1/2}\left(\sqrt{S}\frac{r}{a}\right)\right]\left(\frac{r}{a}\right)^{-3/2}\right\}P_n^1(\cos\vartheta)\mathrm{e}^{st}. \tag{11}$$

From the Stokes equations, we obtain for the integration constants of the pressure

$$sa\rho(n+1)A_n + E_n = 0 \quad \text{and} \quad sa\rho\, nB_n - F_n = 0.$$

3.1. Simple viscous liquid sphere

For a simple viscous liquid sphere (Fig. 1(a)), of which the range $0 \leqslant \vartheta \leqslant \alpha$ is considered to be a rigid wall on $r = a$, the integration constant B_n and D_n vanish together with F_n. The boundary conditions are then given at the rigid cap by

$$u = \upsilon = 0 \quad \text{at } r = a \text{ in the range } 0 \leqslant \vartheta \leqslant \alpha, \tag{12}$$

at the free liquid surface by

$$\tau_{r\vartheta} = \eta\left[r\frac{\partial}{\partial r}\left(\frac{\upsilon}{r}\right) + \frac{1}{r}\frac{\partial u}{\partial\vartheta}\right] = 0 \quad \text{at } r = a \text{ in the range } \alpha < \vartheta \leqslant \pi \tag{13}$$

and

$$\frac{\partial p}{\partial t} - 2\eta\frac{\partial^2 u}{\partial r\partial t} + \frac{\sigma}{a^2}\left\{2u + \frac{1}{\sin\vartheta}\frac{\partial}{\partial\vartheta}\left(\sin\vartheta\frac{\partial u}{\partial\vartheta}\right)\right\} = 0 \quad \text{at } r = a \text{ in the range } \alpha < \vartheta \leqslant \pi. \tag{14}$$

These yield (Eq. (12))

$$\sum_{n=1}^{\infty}\left\{A_n + C_n\mathrm{I}_{n+1/2}(\sqrt{S})\right\}n(n+1)P_n^0(\cos\vartheta) = 0 \quad \text{in the range } 0 \leqslant \vartheta \leqslant \alpha \tag{15}$$

and

$$\sum_{n=1}^{\infty}\left\{A_n(n+1) + C_n\left[\sqrt{S}\mathrm{I}_{n-1/2}(\sqrt{S}) - n\mathrm{I}_{n+1/2}(\sqrt{S})\right]\right\}P_n^1(\cos\vartheta) = 0 \quad \text{in the range } 0 \leqslant \vartheta \leqslant \alpha, \tag{16}$$

while the shear stress-(13) and free surface condition (14) render the results

$$\sum_{n=1}^{\infty}\left\{2A_n(n^2-1)+C_n\left[(S+2n(n+2))\mathrm{I}_{n+1/2}(\sqrt{S})-2\sqrt{S}\mathrm{I}_{n-1/2}(\sqrt{S})\right]\right\}P_n^1(\cos\vartheta)=0$$
$$\text{in the range } \alpha<\vartheta\leqslant\pi \tag{17}$$

and

$$\sum_{n=1}^{\infty}\left\{A_n[S^2+2Sn(n-1)+\sigma^*n(n-1)(n+2)]\right.$$
$$\left.+C_n\left[\sigma^*n(n-1)(n+2)\mathrm{I}_{n+1/2}(\sqrt{S})+2Sn\left(\sqrt{S}\mathrm{I}'_{n+1/2}(\sqrt{S})-\frac{3}{2}\mathrm{I}_{n+1/2}(\sqrt{S})\right)\right]\right\}$$
$$\times P_n^0(\cos\vartheta)=0 \quad \text{in the range } \alpha\leqslant\vartheta\leqslant\pi. \tag{18}$$

In these equations, $\sigma^*\equiv\sigma a/\rho v^2$ is the surface tension parameter. Satisfying these four equations in their respective ranges, yields

$$\sum_{n=1}^{N_1+N_2+1}\{A_n+C_n\mathrm{I}_{n+1/2}(\sqrt{S})\}n(n+1)P_n^0\left[\cos\left(\frac{n_1}{N_1}\alpha\right)\right]=0 \quad \text{for } n_1=0,1,2,\ldots,N_1, \tag{19}$$

$$\sum_{n=1}^{N_1+N_2+1}\{A_n(n+1)+C_n[\sqrt{S}\mathrm{I}_{n-1/2}(\sqrt{S})-n\mathrm{I}_{n+1/2}(\sqrt{S})]\}P_n^1\left[\cos\left(\frac{n_1}{N_1}\alpha\right)\right]=0$$
$$\text{for } n_1=0,1,2,\ldots,N_1 \tag{20}$$

and in the second range

$$\sum_{n=1}^{N_1+N_2+1}\{2A_n(n^2-1)+C_n[(S+2n(n+2))\mathrm{I}_{n+1/2}(\sqrt{S})-2\sqrt{S}\mathrm{I}_{n-1/2}(\sqrt{S})]\}$$
$$\times P_n^1\left[\cos\left(\alpha+\frac{(\pi-\alpha)n_2}{N_2}\right)\right]=0 \quad \text{for } n_2=1,2,\ldots,N_2, \tag{21}$$

$$\sum_{n=1}^{N_1+N_2+1}\left\{A_n[S^2+2Sn(n-1)+\sigma^*n(n-1)(n+2)]+C_n\left[\sigma^*n(n-1)(n+2)\mathrm{I}_{n+1/2}(\sqrt{S})\right.\right.$$
$$\left.\left.+2Sn\left(\sqrt{S}\mathrm{I}'_{n+1/2}(\sqrt{S})-\frac{3}{2}\mathrm{I}_{n+1/2}(\sqrt{S})\right)\right]\right\}P_n^0\left[\cos\left(\alpha+\frac{(\pi-\alpha)n_2}{N_2}\right)\right]=0$$
$$\text{for } n_2=1,2,\ldots,N_2. \tag{22}$$

These are $2(N_1+N_2+1)$ homogeneous algebraic equations in the unknowns $A_1,A_2,\ldots,A_{N_1+N_2+1}$ and $C_1,C_2,\ldots,C_{N_1+N_2+1}$, of which the vanishing coefficient determinant represents the frequency equation for the determination of the lower approximate damped (complex) natural frequencies S_{oN}. In the process to find the zero determinant, we are able to obtain the values of damping $\bar{\sigma}$ and frequency $\bar{\omega}$ as complex values of $S=sa^2/v=\bar{\sigma}\pm\mathrm{i}\bar{\omega}$ which

are contained in the matrix components. To find S_{sol} which makes the determinant zero, we represent diagrams of real part and imaginary part of the determinant with contour lines in a predicted S space where S_{sol} is assumed to exist. From these two diagrams, we can find a solution S_{sol} as a cross-point of zero contour lines of the real and imaginary part of the determinant.

For a simple spherical drop, not being captured in a spherical cap ($\alpha = 0$), the complex frequency equation is given by [10]

$$2(n^2-1)\Big\{[2n(n+2)S-\sigma^* n(n-1)(n+2)]\mathrm{I}_{n+1/2}(\sqrt{S})-2S^{3/2}n\mathrm{I}_{n-1/2}(\sqrt{S})\Big\}$$
$$+\{S^2+2n(n-1)S+\sigma^* n(n-1)(n+2)\}\{[2n(n+2)+S]\mathrm{I}_{n+1/2}(\sqrt{S})-2\sqrt{S}\mathrm{I}_{n-1/2}(\sqrt{S})\}=0,$$

which yields for vanishing viscosity $v \to 0$, the result for a frictionless liquid drop, i.e.,

$$s^2 = -\omega_n^2 = -\frac{\sigma n(n-1)(n+2)}{\rho a^3}$$

and for very large viscosity $v \to \infty$ ($s \to 0$), the two real negative roots

$$s_1 = -\frac{\omega_n^2(2n+1)}{2(n-1)(n+3)v/a^2},$$

$$s_2 = -\frac{2(n-1)(n+3)(2n+5)}{n[2n^2+5n+9]}\frac{v}{a^2}+\frac{\omega_n^2(2n+1)}{2(n-1)(n+3)v/a^2},$$

indicating a strong decay of the liquid motion.

3.2. Spherical viscous drop captured at both poles

For such a system, as shown in Fig. 1(b), the boundary conditions are at the rigid caps

$$u = \upsilon = 0 \quad \text{at } r = a \quad \text{in the range } 0 \leqslant \vartheta \leqslant \alpha, \pi - \alpha \leqslant \vartheta \leqslant \pi, \tag{23}$$

while the shear stress condition and free liquid surface condition have to be satisfied at $r = a$ in the range $\alpha \leqslant \vartheta \leqslant \pi - \alpha$. This yields for the determination of the approximate complex frequencies from Eq. (23).

$$\sum_{n=1}^{N_1+N_2+N_3+1}\{A_n + C_n\mathrm{I}_{n+1/2}(\sqrt{S})\}n(n+1)P_n^0\left[\cos\left(\frac{n_1}{N_1}\alpha\right)\right] = 0 \quad \text{for } n_1 = 0,1,2,\ldots,N_1, \tag{24}$$

$$\sum_{n=1}^{N_1+N_2+N_3+1}\left\{A_n(n+1)+C_n\left[\sqrt{S}\mathrm{I}_{n-1/2}(\sqrt{S})-n\mathrm{I}_{n+1/2}(\sqrt{S})\right]\right\}P_n^1\left[\cos\left(\frac{n_1}{N_1}\alpha\right)\right] = 0$$
$$\text{for } n_1 = 0,1,2,\ldots,N_1, \tag{25}$$

$$\sum_{n=1}^{N_1+N_2+N_3+1}\{A_n + C_n\mathrm{I}_{n+1/2}(\sqrt{S})\}n(n+1)P_n^0\left[\cos\left(\pi-\frac{n_2}{N_2}\alpha\right)\right] = 0 \quad \text{for } n_2 = 0,1,2,\ldots,N_2, \tag{26}$$

$$\sum_{n=1}^{N_1+N_2+N_3+1}\{A_n(n+1)+C_n[\sqrt{S}\mathrm{I}_{n-1/2}(\sqrt{S})-n\mathrm{I}_{n+1/2}(\sqrt{S})]\}P_n^1\left[\cos\left(\pi-\frac{n_2}{N_2}\alpha\right)\right]=0$$
$$\text{for } n_2=0,1,2,\ldots,N_2 \tag{27}$$

and for the shear stress and free surface condition from Eqs. (13) and (14)

$$\sum_{n=1}^{N_1+N_2+N_3+1}\{2A_n(n^2-1)+C_n[(S+2n(n+2))\mathrm{I}_{n+1/2}(\sqrt{S})-2\sqrt{S}\mathrm{I}_{n-1/2}(\sqrt{S})]\}$$
$$\times P_n^1\left[\cos\left(\alpha+\frac{(\pi-2\alpha)n_3}{N_3}\right)\right]=0 \quad \text{for } n_3=1,2,\ldots,N_3-1, \tag{28}$$

$$\sum_{n=1}^{N_1+N_2+N_3+1}\left\{A_n[S^2+2Sn(n-1)+\sigma^*n(n-1)(n+2)]+C_n\left[\sigma^*n(n-1)(n+2)\mathrm{I}_{n+1/2}(\sqrt{S})\right.\right.$$
$$\left.\left.+2Sn\left(\sqrt{S}\mathrm{I}'_{n+1/2}(\sqrt{S})-\frac{3}{2}\mathrm{I}_{n+1/2}(\sqrt{S})\right)\right]\right\}P_n^0\left[\cos\left(\alpha+\frac{(\pi-2\alpha)n_3}{N_3}\right)\right]=0$$
$$\text{for } n_3=1,2,\ldots,N_3-1. \tag{29}$$

These are $2(N_1+N_2+N_3+1)$ homogeneous algebraic equations for the determination of the lower approximate complex frequencies, being obtained from the vanishing coefficients determinant of order $2(N_1+N_2+N_3+1)$. Mode shapes and natural frequencies of a system of frictionless liquid may be found in Ref. [17].

3.3. Annular viscous spherical liquid system

If an annular liquid of volume $V_0=4\pi a^3/3(1-k^3)(k\equiv b/a)$ is placed around a spherical center core of radius b and in addition captured at $r=a$ in the range $0\leqslant\vartheta\leqslant\alpha$ (Fig. 1(c)), the boundary conditions are given for the rigid center core by

$$u=\upsilon=0 \quad \text{at } r=b \text{ and all } \vartheta \text{ (Fig. 1(c), } 0\leqslant\vartheta\leqslant\pi) \tag{30}$$

and for the rigid cap by

$$u=\upsilon=0 \quad \text{at } r=a \text{ in the range } 0\leqslant\vartheta\leqslant\alpha. \tag{31}$$

The shear stress condition at the free surface is (13), i.e.,

$$\tau_{r\vartheta}=0 \quad \text{at } r=a \text{ in the range } \alpha<\vartheta\leqslant\pi \tag{32}$$

and the free surface condition is Eq. (14). We obtain with the velocity distribution

$$u(r,\vartheta,t)=\sum_{n=1}^{\infty}n(n+1)\left\{A_n\left(\frac{r}{a}\right)^{n-1}+B_n\left(\frac{r}{a}\right)^{-(n+2)}+C_n\left(\frac{r}{a}\right)^{-3/2}\mathrm{I}_{n+1/2}\left(\sqrt{S}\frac{r}{a}\right)\right.$$
$$\left.+D_n\left(\frac{r}{a}\right)^{-3/2}\mathrm{K}_{n+1/2}\left(\sqrt{S}\frac{r}{a}\right)\right\}P_n^0(\cos\vartheta)\mathrm{e}^{st}$$

and

$$\upsilon(r,\vartheta,t)=\sum_{n=1}^{\infty}\Bigg\{A_n(n+1)\Big(\frac{r}{a}\Big)^{n-1}-B_n n\Big(\frac{r}{a}\Big)^{-(n+2)}+C_n\Big[\frac{r}{a}\sqrt{S}\mathrm{I}_{n-1/2}\Big(\sqrt{S}\frac{r}{a}\Big)-n\mathrm{I}_{n+1/2}\Big(\sqrt{S}\frac{r}{a}\Big)\Big]\Big(\frac{r}{a}\Big)^{-3/2}-D_n\Big[\frac{r}{a}\sqrt{S}\mathrm{K}_{n-1/2}\Big(\sqrt{S}\frac{r}{a}\Big)+n\mathrm{K}_{n+1/2}\Big(\sqrt{S}\frac{r}{a}\Big)\Big]\times\Big(\frac{r}{a}\Big)^{-3/2}\Bigg\}P_n^1(\cos\vartheta)\mathrm{e}^{st},$$

from $u=\upsilon=0$ at $r=b$, the expressions

$$A_n k^{n+1/2}+B_n k^{-(n+1/2)}+C_n\mathrm{I}_{n+1/2}(k\sqrt{S})+D_n\mathrm{K}_{n+1/2}(k\sqrt{S})=0, \tag{33}$$

$$A_n(n+1)k^{n+1/2}-B_n n k^{-(n+1/2)}+C_n\Big[k\sqrt{S}\mathrm{I}_{n-1/2}(k\sqrt{S})-n\mathrm{I}_{n+1/2}(k\sqrt{S})\Big]-D_n\Big[k\sqrt{S}\mathrm{K}_{n-1/2}(k\sqrt{S})+n\mathrm{K}_{n+1/2}(k\sqrt{S})\Big]=0, \tag{34}$$

from which C_n and D_n may be obtained as functions of A_n and B_n. At the free surface, we obtain for the range $0\leqslant\vartheta\leqslant\alpha$ from Eq. (31) in the range $0\leqslant\vartheta\leqslant\alpha$:

$$\sum_{n=1}^{N_1+N_2+1}n(n+1)\{A_n+B_n+C_n\mathrm{I}_{n+1/2}(\sqrt{S})+D_n\mathrm{K}_{n+1/2}(\sqrt{S})\}P_n^0\Big[\cos\Big(\frac{n_1}{N_1}\alpha\Big)\Big]=0 \quad \text{for } n_1=0,1,2,\ldots,N_1, \tag{35}$$

$$\sum_{n=1}^{N_1+N_2+1}\{A_n(n+1)-B_n n+C_n[\sqrt{S}\mathrm{I}_{n-1/2}(\sqrt{S})-n\mathrm{I}_{n+1/2}(\sqrt{S})]-D_n[\sqrt{S}\mathrm{K}_{n-1/2}(\sqrt{S})+n\mathrm{K}_{n+1/2}(\sqrt{S})]\}P_n^1\Big[\cos\Big(\frac{n_1}{N_1}\alpha\Big)\Big]=0 \quad \text{for } n_1=0,1,2,\ldots,N_1 \tag{36}$$

and for the range $\alpha\leqslant\vartheta\leqslant\pi$ from Eq. (32):

$$\sum_{n=1}^{N_1+N_2+1}\Bigg\{2(n^2-1)A_n+2n(n+2)B_n+C_n\Big[S\mathrm{I}'_{n-1/2}(\sqrt{S})-\frac{3\sqrt{S}}{2}\mathrm{I}_{n-1/2}(\sqrt{S})-n\sqrt{S}\mathrm{I}'_{n+1/2}(\sqrt{S})+n\Big(n+\frac{7}{2}\Big)\mathrm{I}_{n+1/2}(\sqrt{S})\Big]-D_n\Big[S\mathrm{K}'_{n-1/2}(\sqrt{S})-\frac{3\sqrt{S}}{2}\mathrm{K}_{n-1/2}(\sqrt{S})+n\sqrt{S}\mathrm{K}'_{n+1/2}(\sqrt{S})-n\Big(n+\frac{7}{2}\Big)\mathrm{K}_{n+1/2}(\sqrt{S})\Big]\Bigg\}P_n^1\Big[\cos\Big(\alpha+\frac{(\pi-\alpha)n_2}{N_2}\Big)\Big]=0 \quad \text{for } n_2=1,2,\ldots,N_2 \tag{37}$$

and from Eq. (14):

$$\sum_{n=1}^{N_1+N_2+1} \{A_n[(n+1)S^2+2n(n^2-1)S+\sigma^* n(n^2-1)(n+2)] + B_n[\sigma^* n(n^2-1)(n+2)-S^2 n-2Sn(n+1)(n+2)] + C_n[2S\sqrt{S}n(n+1)\mathrm{I}'_{n+1/2}(\sqrt{S})-3Sn(n+1)\mathrm{I}_{n+1/2}(\sqrt{S})+\sigma^* n(n^2-1)(n+2)\mathrm{I}_{n+1/2}(\sqrt{S})] + D_n[2S\sqrt{S}n(n+1)\mathrm{K}'_{n+1/2}(\sqrt{S})-3Sn(n+1)\mathrm{K}_{n+1/2}(\sqrt{S})+\sigma^* n(n^2-1)(n+2) \times \mathrm{K}_{n+1/2}(\sqrt{S})]\} \times P_n^0\left[\cos\left(\alpha+\frac{(\pi-\alpha)n_2}{N_2}\right)\right]=0 \quad \text{for } n_2=1,2,\ldots,N_2. \tag{38}$$

These are $2(N_1+N_2+1)$ homogeneous algebraic equations, which after the determination of C_n and D_n from Eqs. (33) and (34) exhibit the unknowns A_n and B_n. The vanishing of the determinant represents the complex frequency equation for the determination of S_{oN}. Mode shapes and natural frequencies of a system of frictionless liquid may be found in Ref. [17].

4. Translational excitation

If the spherical wall is harmonically excited with $Z_0 e^{i\Omega t}$ in z direction, the captured liquid drop (Fig. 1(a)) will respond in axisymmetric motion ($\partial/\partial\varphi = 0, w = 0$). The pressure distribution is then given by

$$p(r,\vartheta,t) = p_0 - \rho\Omega^2 Z_0 e^{i\Omega t} r\cos\vartheta + \bar{p}(r,\vartheta,t). \tag{39}$$

With the solution (9) of the differential equation of the stream function, we obtain with the boundary condition $u=0$ (Eq. (15)), $v=0$ (Eq. (16)), and the shear stress condition $\tau_{r\vartheta}=0$ (Eq. (17)) together with combined free surface equation ($i\Omega a^2/v \equiv \Omega^*$),

$$\sum_{n=1}^{N_1+N_2+1} \left\{ A_n(n+1)[\Omega^{*2}+2\Omega^{*2}n(n-1)+\sigma^* n(n-1)(n+2)] + C_n n(n+1)\left[\sigma^*(n-1)(n+2)\mathrm{I}_{n+1/2}(\sqrt{\Omega^*})+2\Omega^*\left(\sqrt{\Omega^*}\mathrm{I}'_{n+1/2}(\sqrt{\Omega^*})-\frac{3}{2}\mathrm{I}_{n+1/2}(\sqrt{\Omega^*})\right)\right]\right\} \times P_n^0\left[\cos\left(\alpha+\frac{(\pi-\alpha)n_2}{N_2}\right)\right] = \Omega^{*3}\bar{Z}_0\cos\left(\alpha+\frac{(\pi-\alpha)n_2}{N_2}\right) \quad \text{in the range } \alpha\leqslant\vartheta\leqslant\pi, \quad n_2=1,2,\ldots,N_2, \tag{40}$$

the equations of response, where $\sigma^* \equiv \sigma a/\rho v^2$ and $\bar{Z}_0 \equiv Z_0 v/a^2$. Eqs. (19)–(21) and (40) represent an algebraic inhomogeneous system of $2(N_1+N_2+1)$ equations for the determination of the response values $A_j(\Omega_1^*)$ and $C_j(\Omega_1^*)$, $j=1,2,\ldots,N_1+N_2+1$. The free surface response is

obtained from

$$\left|\frac{\zeta}{\bar{Z}_0}\right| = \frac{1}{\Omega^* \bar{Z}_0} \sum_{n=1}^{\infty} \{A_n + C_n \mathrm{I}_{n+1/2}(\sqrt{\Omega^*})\} n(n+1) P_n^0(\cos\vartheta) \tag{41}$$

where ζ represents the free surface displacement.

5. Numerical evaluations and conclusions

Some of the above-obtained analytical results have been evaluated numerically. Only the configuration of a captured drop in a simple rigid cap (Fig. 1(a)) of $0 \leqslant \vartheta \leqslant \alpha$ has been treated numerically here with $\bar{\alpha}(\equiv \alpha/\pi) = 0, 0.1, 0.3$ and 0.5 for various liquid surface tensions $\sigma^* = \sigma a/\rho v^2$. Instead of the surface parameter σ^*, we could either write the capillary Reynolds number $\tilde{R}e_\sigma = \sqrt{\sigma^*}$ or the Ohnesorge number Oh, often used by the scientific community of zero- or microgravity research. The Ohnesorge number is $Oh = 1/\sqrt{\sigma^*}$ or the reciprocal of the capillary Reynolds number, i.e. $Oh = (\tilde{R}e_\sigma)^{-1} = (\rho v^2/\sigma a)^{1/2}$. In the numerical calculations, the numbers of unknown parameters, A_n and B_n, were taken to be 70, i.e., $n = N_1 + N_2 + 1 = 70$, respectively, to obtain reliable engineering data. And numbers of $(N_1 + 1)$ and N_2 were taken to be proportional to the ratio of the captured and uncaptured regions, $\bar{\alpha}$ and $(1 - \bar{\alpha})$.

For reference, the vibration modes of a simple captured liquid system for various $\bar{\alpha}$ and mode numbers n [17] are shown in Fig. 2. First of all, we find in Table 1 the damped natural frequencies for the modes $n = 1, 2$ and 3, for $\sigma^* = 100\,(\tilde{R}e_\sigma = 10)$ and $500\,(\tilde{R}e_\sigma = 22.36)$, comparing the inviscid and viscous results. It may be noticed that the viscous results nearly always exhibit smaller magnitude than the inviscid cases. In addition, the difference of them is increasing with increasing $\bar{\alpha} = \alpha/\pi$ for the presented small σ^* ($\sigma^* = 100, 500$; or $\tilde{R}e_\sigma = 10, 22.36$).

In Fig. 3, we exhibit the complex frequency of the liquid of the simple-sphere-cap case for surface tension parameters $\sigma^* = 100$ ($\tilde{R}e_\sigma = 10$), 500 ($\tilde{R}e_\sigma = 22.36$) and 1000 ($\tilde{R}e_\sigma = 31.62$). With increasing rigid cap magnitude $\bar{\alpha}$, the natural damped oscillation frequency $\mathrm{Im}\, S \equiv \bar{\omega} a^2/v$ increases. The decay magnitude of the oscillation $|\mathrm{Re}\, S| \equiv \bar{\sigma} a^2/v$ increases as $\bar{\alpha}$ increases, indicating that with larger cap $\bar{\alpha}$ the damped oscillations decay more rapidly. This is true for the modes $n = 2$ and 3, as shown in Fig. 3. For $n = 1$ we notice at certain $\bar{\alpha}$-values an instability, where $\mathrm{Re}\, S$ assumes positive values. It may be seen in Fig. 3(a) that for $\sigma^* = 100\,(\tilde{R}e_\sigma = 10)$ stability is preserved in the here presented total $\bar{\alpha}$-range. For increased σ^*, i.e., $\sigma^* = 500$ ($\tilde{R}e_\sigma = 22.36$), the range $0.113 < \bar{\alpha} < 0.367$ exhibits for $n = 1$ instability (see Fig. 3(b)), while a further increased surface tension parameter $\sigma^* = 1000\,(\tilde{R}e_\sigma = 31.62)$ shows for the mode $n = 1$ instability in the $\bar{\alpha}$-range $0.122 < \bar{\alpha} < 0.475$ (Fig. 3(c)). With these results, we notice that with increasing surface tension parameter σ^* or increasing capillary Reynolds number $\tilde{R}e_\sigma$, the range of instability increases, exhibiting for the lower values a small increase of the cap angle and a larger increase of the cap angle for larger values. The limits of the instability region show for the lower limit with the increase of σ^* a much smaller regional increase than for the upper limit. This indicates that for large $\sigma^* \equiv \sigma a \rho/\eta^2$, i.e. for large surface tension σ, large radius a and/or large density ρ and small dynamic viscosity $\eta(\sim \eta^2)$, the here chosen equilibrium position of spherical geometry no longer represents a stable configuration of the liquid. This has also been detected in some unpublished

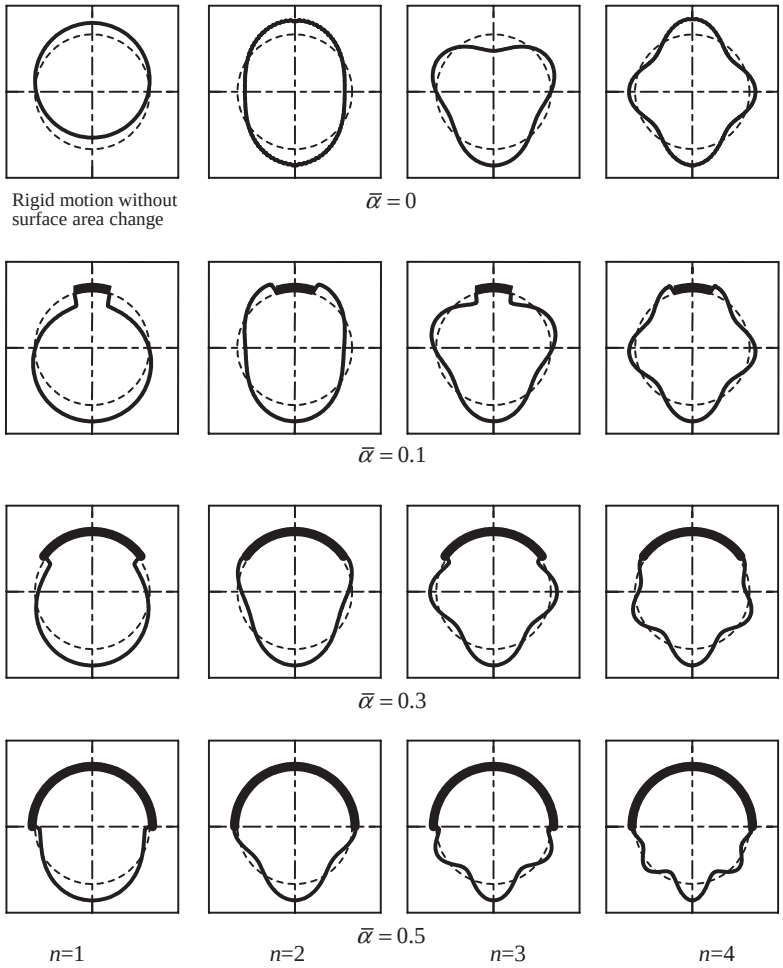

Fig. 2. Vibration modes for simple captured liquid system for various $\bar{\alpha}$ and mode number n [17].

Table 1
Comparison of the damped natural frequency with that of a frictionless drop

σ^* ($\tilde{R}e_\sigma$)	100 (10)						500 (22.36)					
	$n=1$		$n=2$		$n=3$		$n=1$		$n=2$		$n=3$	
$\bar{\alpha}$	Viscous	Inviscid	Viscous	Inviscid	Viscous	Inviscid	Viscous	Inviscid	Viscous	Inviscid	Viscous	Inviscid
0	0	0	27.5	28.3	51.9	54.8	0	0	62.7	63.2	120.4	122.5
0.1	6.97	4.04	32.9	30.8	60.8	59.9	16.9	9.03	76.4	68.9	142.0	134.0
0.3	21.7	11.9	56.8	45.2	96.0	87.0	46.6	26.7	128.0	101.2	223.0	194.6
0.5	40.1	25.9	96.6	78.7	156.0	148.5	88.0	57.8	223.0	175.9	372.0	332.2

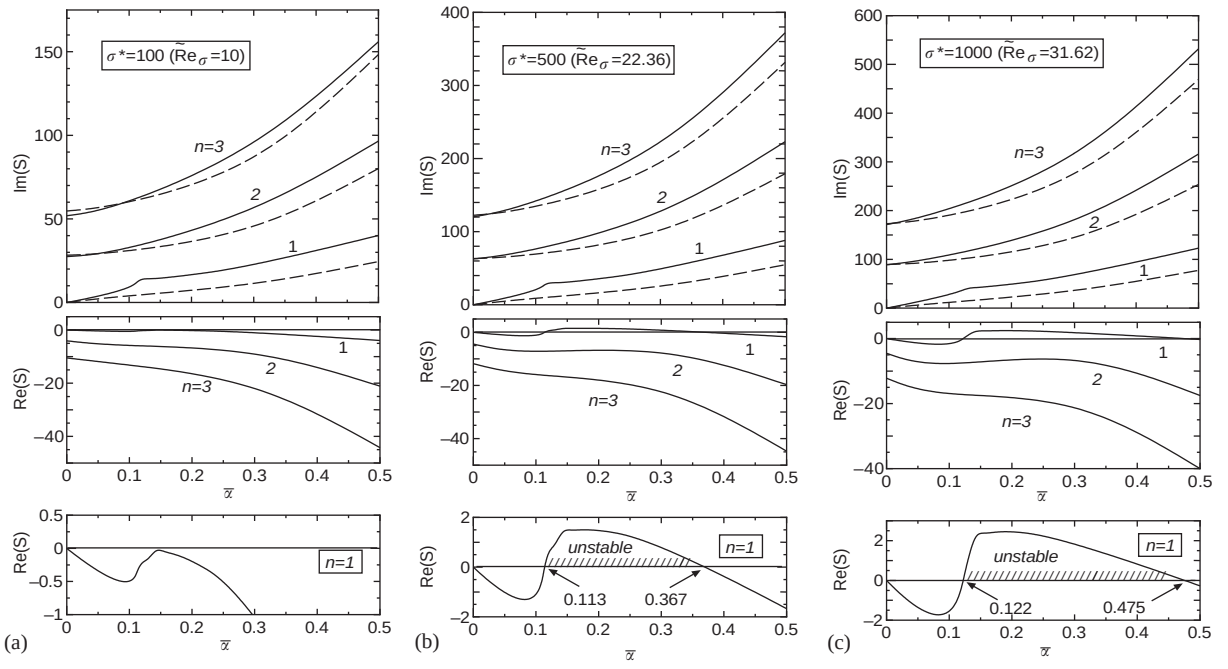

Fig. 3. Complex frequencies of a simple sphere with cap angle $\bar{\alpha}$, $n = 1, 2, 3$: - - -, inviscid drop; (a) $\sigma^* = 100$ ($\tilde{Re}_\sigma = 10$), all n: always stable; (b) $\sigma^* = 500$ ($\tilde{Re}_\sigma = 22.36$), $n = 1 : 0.113 < \bar{\alpha} < 0.367$ unstable; (c) $\sigma^* = 1000$ ($\tilde{Re}_\sigma = 31.62$), $n = 1 : 0122 < \bar{\alpha} < 0.475$ unstable.

experiments with water where the Bond numbers exhibited the magnitude $Bo = 0.54$ and where the liquid could not maintain a spherical geometry. For smaller σ^*-values, however, the totally embedded configuration is possible and exhibits the oscillatory- and decay behavior presented in the shown Fig. 3. The dashed line represents the non-viscous case, as presented in Ref. [17]. We notice that for small $\sigma^*(\tilde{Re}_\sigma)$ (here $\sigma^* = 100$) the oscillation frequency of the viscous case is for small $\bar{\alpha}$, i.e., small cap size, slightly smaller than that for inviscid liquid. For larger magnitudes of $\bar{\alpha}$, the inviscid frequencies are always smaller than those of the viscous liquid. This phenomenon disappears for larger liquid surface tension parameter σ^*, here case (b) $\sigma^* = 500$ ($\tilde{Re}_\sigma = 22.36$) and (c) $\sigma^* = 1000$ ($\tilde{Re}_\sigma = 31.62$). In addition, we may notice that the case $\bar{\alpha} = 0$ results in the same values as obtained in Ref. [10]. The results presented in Fig. 3 show that the oscillation frequencies increase with increasing liquid surface tension σ^* or increasing capillary Reynolds number $\tilde{Re}_\sigma$, while the decay magnitude exhibits only a slight decrease with the increase of σ^*. This may also be found in Ref. [10] for $\bar{\alpha} = 0$, i.e., the free liquid sphere without a cap. For the mode $n = 1$, the value of Re S fluctuates in a range of small magnitude around the stability boundary $\mathrm{Re}\, S = 0$ and exhibits slightly increasing decay magnitude for increasing $\bar{\alpha}$-values, as soon as the instability region has been passed.

In Fig. 4, we exhibit the change of the complex frequencies as a function of the variation of the liquid surface tension σ^* or capillary Reynolds number $\tilde{Re}_\sigma$ for various captured drops, i.e., for $\bar{\alpha} = 0$ (no cap, Fig. 4(a)) and $\bar{\alpha} = 0.1$ (Fig. 4(b)), 0.3 (Fig. 4(c)) and 0.5 (Fig. 4(d)). The case $\bar{\alpha} = \alpha/\pi = \frac{1}{2}$ represents a liquid sphere of which only half of the surface is free to oscillate. For a

free liquid drop $\bar{\alpha} = 0$ (Fig. 4(a)), we notice that with increasing liquid surface tension σ^* (or $\tilde{Re}_\sigma$), an increase of the oscillation frequencies $\bar{\omega}a^2/\nu$ and a slight increase of the decay magnitude $|\bar{\sigma}a^2/\nu|$ occurs. This is more pronounced for higher oscillation modes ($n = 3, 4$). The origin 0 represents the mode $n = 1$, i.e., $\bar{\sigma}a^2/\nu = \bar{\omega}a^2/\nu = 0$, representing nothing but the rigid body motion of the spherical drop with unchanged free liquid surface area. This was found in Ref. [17] for $\bar{\alpha} = 0$ Ref. [17, Figs. 3 and 4]. In Fig. 4(b), the complex frequencies are presented for a small cap area $\bar{\alpha} = 0.1(\alpha = \pi/10)$. We detect similar behavior as for a free spherical drop, i.e., increasing oscillation frequency and increasing decay magnitude as the liquid surface tension σ^* increases from $\sigma^* = 100$ to 1000. The difference to the case $\bar{\alpha} = 0$ is that the mode $n = 1$ appears and shows, for its oscillation- and decay, behavior the dependency of the surface tension parameter σ^* or capillary Reynolds number $\tilde{Re}_\sigma$. In the evaluated σ^*-range, the frequency and the decay increase with σ^* and remain in the stable region. For $\bar{\alpha} = 0.3$, the complex frequencies are presented in Fig. 4(c). Here we notice a change of the course for increasing σ^*. In the oscillation mode $n = 2$, the increase of the liquid surface tension results as before in an increase of the oscillation frequency,

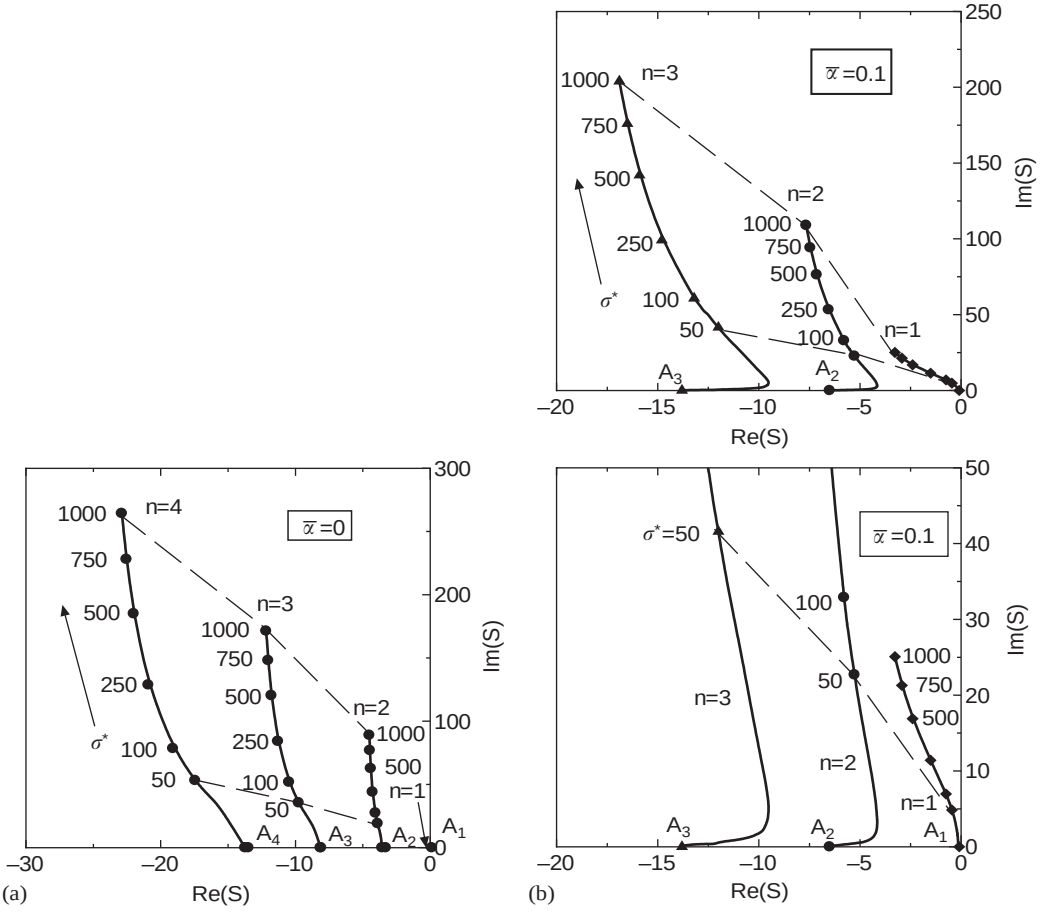

Fig. 4. Variations of complex frequencies of a simple liquid sphere with surface tension σ^* (capillary Reynolds number ranges up to $\tilde{Re}_\sigma = 31.62$): (a) $\bar{\alpha} = 0$; (b) $\bar{\alpha} = 0.1$; (c) $\bar{\alpha} = 0.3$; (d) $\bar{\alpha} = 0.5$.

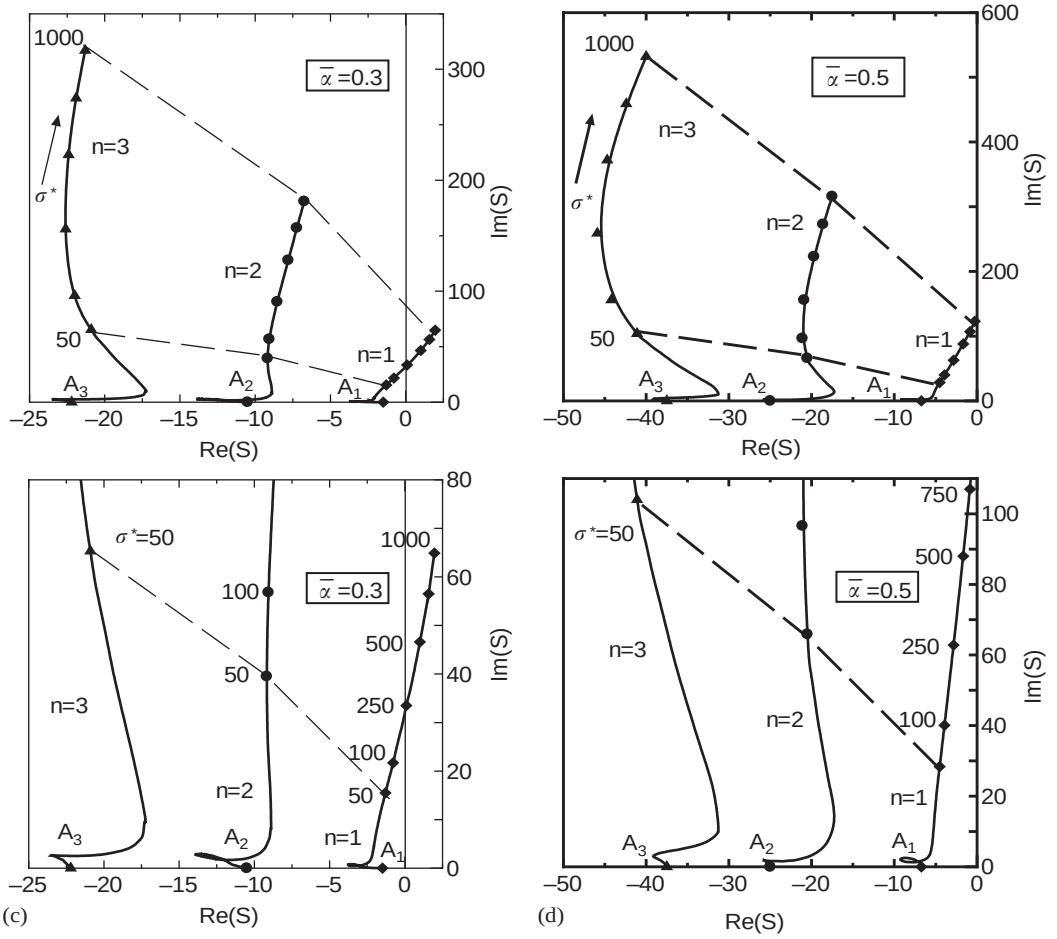

Fig. 4. (*Continued*)

but a decrease of the decay magnitude. For a larger oscillation mode $n = 3$, we note first an increase and then a decrease of the decay magnitude as σ^* increases. The mode $n = 1$ becomes unstable, as it moves for increased σ^* into the region $\mathrm{Re}\,S > 0$. A closer look at the numerical evaluation also reveals that for very small σ^*-values a loop appears in the curves, indicating that an increase of σ^* yields first an increase of the damped frequency, as well as the decay magnitude, while a further increase of σ^* renders smaller damped frequencies and smaller decay. This phenomenon disappears as $\bar{\alpha}$ decreases, i.e., for cap values becoming smaller. Whether this phenomenon is based on a physical or numerical effect could not be cleared. This is also exhibited for $\bar{\alpha} = 0.5$, where half of the spherical surface is permitted to oscillate. The mode $n = 1$ shows with increasing liquid surface tension or increasing capillary Reynolds number $\tilde{R}e_\sigma$, also an increase of the oscillation frequency and a decrease of the decay magnitude $|\bar{\sigma}a^2/\nu|$ in the given range of σ^*, i.e., $50 \leqslant \sigma^* \leqslant 1000$. Only in the very low σ^*-range, the decay magnitude decreases rapidly with a slight increase of σ^* (Fig. 4(d)).

It may be noticed, that according to Refs. [9,10], the oscillation for the case $\bar{\alpha}=0$ ceased to exist at $\bar{\omega}a^2/\nu=\mathrm{Im}\,S=0$ (double root) for $\bar{\sigma}a^2/\nu=-3.57$ and $\sigma^*=\sigma a/\rho\nu^2=1.70$ (i.e. $\tilde{R}e_\sigma=1.3$) for $n=2$ (see A_2 in Fig. 4(a)), $\bar{\sigma}a^2/\nu=-8.15$ and $\sigma^*=2.59$ (i.e. $\tilde{R}e_\sigma=1.61$) for $n=3$ (see A_3 in Fig. 4(a)) and $\bar{\sigma}a^2/\nu=-13.74$ and $\sigma^*=3.31$ (i.e. $\tilde{R}e_\sigma=1.82$) for $n=4$ (see A_4 in Fig. 4(a)), thus indicating only the possibility for an aperiodic motion. There shall exist similar values for $\bar{\alpha}\neq 0$ as the trend and the indicated points $A_j(j=1,2,3)$ of the curves in the results of Fig. 4 exhibit.

In Table 2, we represent the critical surface tension parameter σ^* together with the decay magnitude $\bar{\sigma}a^2/\nu$ for the modes $n=1,2,3$. The first line for $\bar{\alpha}=0$ (i.e. no cap) confirms the previous results [10]. The remaining results for ceasing oscillations, i.e. an aperiodic motion, represent in the first column the magnitude of the decay at A_1, while the second column shows the σ_1^*-value at that location. Similar results are given in the third and fourth column for $n=2$ and in the fifth and sixth column for $n=3$ (see also Fig. 4).

In Fig. 5, we show the change of the complex frequencies as a function of the cap angle $\bar{\alpha}$ as a parameter for $n=1,2$ and 3, where the changes of σ^* are marked by points. In this figure, the variation of the complex frequencies for the modes $n=1,2,3$ with the change of the cap angle $\bar{\alpha}$ are presented. The results for the mode $n=1$ is shown in Fig. 5(a), where we notice for various $\bar{\alpha}$- and σ^*-value the penetration into the instability region. The modes $n=2$ and 3 remain for the presented σ^*-range in the stable area. We notice that the increase of the cap angle $\bar{\alpha}$ from $\bar{\alpha}=0.1$ to 0.3, the spherical liquid shape remains stable until the surface tension parameter σ^* reaches the value of $\sigma^*\geqslant 235$ (i.e. $\tilde{R}e_\sigma=15.33$). If the cap angle is such that half of the globule is embedded in the cap, i.e., $\bar{\alpha}=1/2$, the spherical shape remains stable until σ^* reaches the magnitude of about $\sigma^*\geqslant 1094$ (i.e. $\tilde{R}e_\sigma=33.07$).Thus, with increasing cap angle $\bar{\alpha}$, the range of stability of a spherical drop is guaranteed for relatively large σ^* or $\tilde{R}e_\sigma$. It is, in the here treated $\bar{\alpha}$- and σ^*-range, always the mode $n=1$ that makes the system for some values $\bar{\alpha}$ and σ^* unstable. For the modes $n=2$ and 3, the captured drop remains for the investigated σ^* or $\tilde{R}e_\sigma$-values in the stable region (see Fig. 5(b)).

To exhibit for the mode $n=1$, for which the captured liquid sphere becomes unstable, the region of instability we show in Fig. 6 the values σ^* and the imaginary part $\mathrm{Im}\,S_{\mathrm{crit}}$ at which instability sets in, i.e., $\mathrm{Re}\,S=0$. The marked area represents the domain of instability for $\bar{\alpha}$ and $\sigma^*_{\mathrm{crit}}(\tilde{R}e_{\sigma\mathrm{crit}})$, while the dashed curve is the critical imaginary part as a function of σ^*_{crit} and $\bar{\alpha}$. Finally, Fig. 7 represents the critical surface tension parameter σ^*_{crit} together with the critical decay value $\mathrm{Re}\,S_{\mathrm{crit}}$ for these modes $n=1,2,3$ as functions of the cap angle $\bar{\alpha}$ for the aperiodic motion ($\mathrm{Im}\,S=0$) of the captured spherical drop. This behavior has already been detected in a freely floating sphere [10] and appears also here in a restrained drop. Each mode exhibits, in comparison with the unrestrained drop, increased decay magnitude as the cap angle $\bar{\alpha}$ increase and also increased decay as the mode number becomes higher. The corresponding surface tension

Table 2
Critical surface tension parameter

$\bar{\alpha}$	$\bar{\sigma}_1a^2/\nu$	σ_1^*	$\bar{\sigma}_2a^2/\nu$	σ_2^*	$\bar{\sigma}_3a^2/\nu$	σ_3^*
0	—	—	−3.57	1.70	−8.15	2.59
0.1	−0.094	0.0094	−6.48	0.769	−13.8	1.60
0.3	−1.49	0.043	−10.5	0.31	−22.2	0.649
0.5	−6.73	0.172	−25.0	0.71	−37.5	1.05

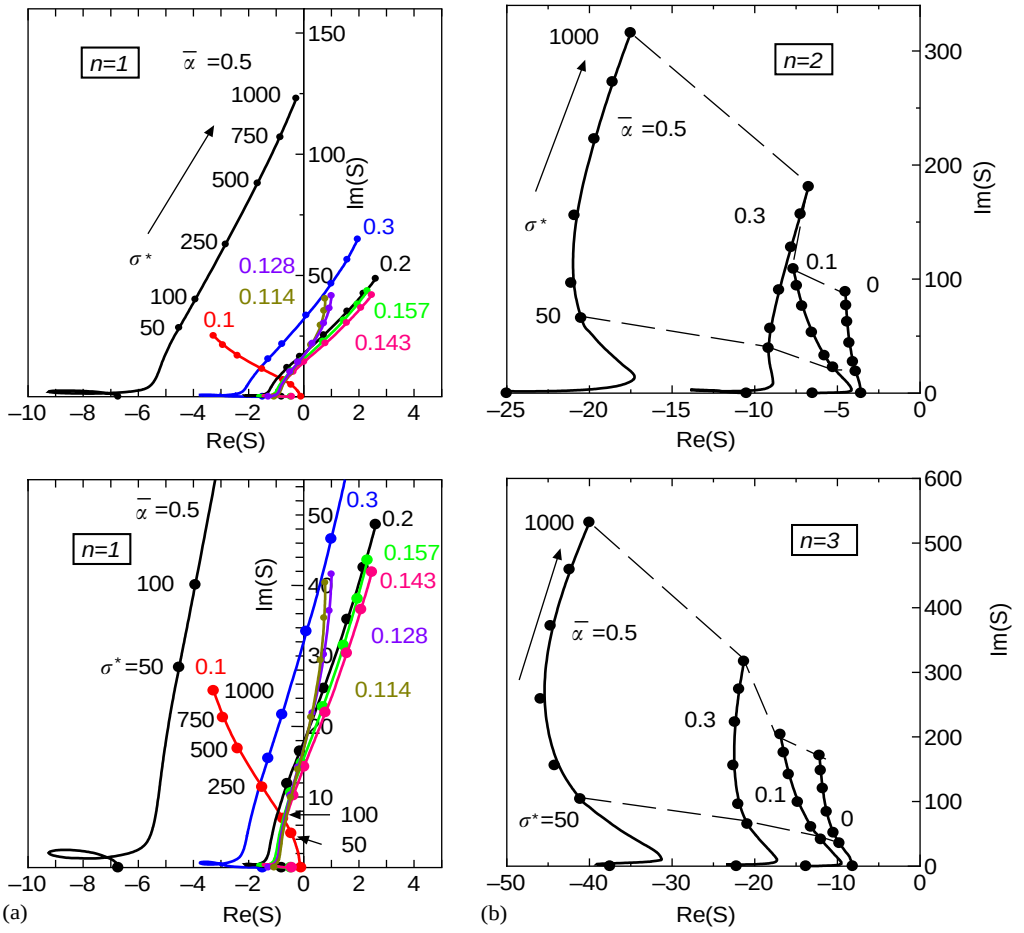

Fig. 5. Variations of complex frequencies of a simple liquid sphere with cap angle $\bar{\alpha}$ (capillary Reynolds number ranges up to $\tilde{Re}_\sigma = 31.62$): (a) $n = 1$; (b) $n = 2, 3$.

parameter is also presented in Fig. 7. It may be mentioned that an experimental attempt for small captured drop of water, exhibiting a Bond number $Bo = \rho g a^2/\sigma = 0.54$ failed, since the liquid could not assume the spherical equilibrium geometry. This is caused by the large $\sigma^* > 10^4$ of the test fluid water. Similar experiments have shown the same phenomena, the results of which were reported in Ref. [18], where the natural frequency of a constrained drop of density ρ_1 immersed in another liquid of density ρ_2 (close to ρ_1) could only be measured for lower $\bar{\alpha}$-values, and where instability occurred in the other cases.

6. Conclusions

Under the assumption of small liquid surface deformations and of zero gravity, the axisymmetric oscillations of a captured viscous liquid sphere have been treated. The liquid

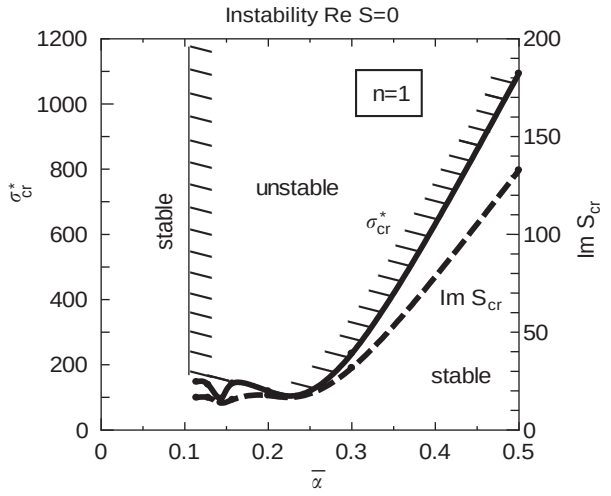

Fig. 6. Critical surface tension σ^* and $\mathrm{Im}\, S_{\mathrm{crit}}$ with cap angle $\bar{\alpha}$ for instability $\mathrm{Re}\, S = 0$, $n = 1$ (critical capillary Reynolds number ranging from $\tilde{R}e_\sigma = 0$ to 34.64).

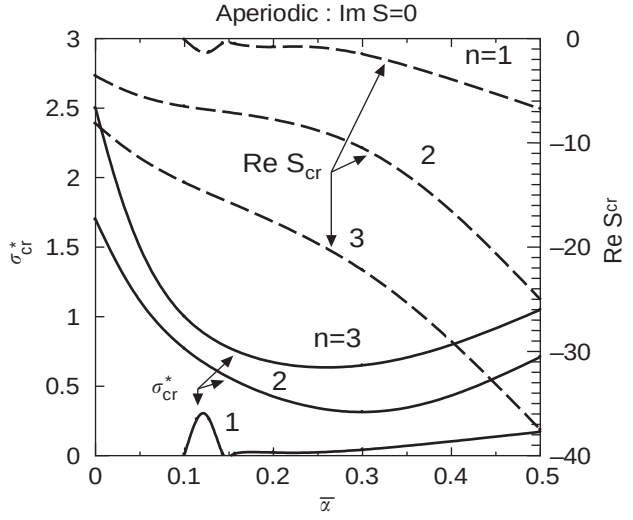

Fig. 7. Critical surface tension σ^* and $\mathrm{Re}\, S_{\mathrm{crit}}$ with cap angle $\bar{\alpha}$ for aperiodic motion with $\mathrm{Im}\, S = 0$, $n = 1, 2, 3$ (critical capillary Reynolds number ranging from $\tilde{R}e_\sigma = 0$ to 1.732).

behavior—being partially in contact with a spherical cap of equal diameter—is determined for engineering estimates, yielding oscillation frequencies and decay magnitudes for various liquid modes, as functions of the cap angle $\bar{\alpha}$ and the surface tension parameter $\sigma^* \equiv \sigma a/\rho\nu^2$ or capillary Reynolds number $\tilde{R}e_\sigma = \sqrt{\sigma^*}$.

The following results have been obtained:

1. The solid cap support changes, with increasing cap angle $\bar{\alpha}$, the damped oscillation frequencies and decay values to larger magnitudes. This is also valid for higher modes.
2. While the unrestrained spherical liquid globule exhibits for $n = 1$ zero natural frequency, describing a rigid body motion of the liquid sphere without change of the free liquid surface area, the captured drop shows a new low-frequency mode. This is valid for frictionless and viscous liquid as well.
   This mode $n = 1$ approaches for vanishing cap angle the rigid body mode with vanishing oscillation frequency, while the higher modes $n \geqq 2$ assume those mode shapes previously obtained by Lamb.
3. It was detected that, in contrast to the unrestrained drop, the drop embedded in a spherical cap ceases to be stable for the new low-frequency mode $n = 1$, depending on the magnitude of the cap angle $\bar{\alpha}$ and the liquid surface tension or capillary Reynolds number. This indicates that the assumed spherical shape is no longer a valid geometry of equilibrium for some captured drops. With the increase of the surface tension σ^* or $\tilde{R}e_\sigma$, the instability region of the mode $n = 1$ increases. As the cap angle $\bar{\alpha}$ increases, the range of σ^* of stability for a spherical equilibrium shape increase too. For small $\bar{\alpha}$, stability is only guaranteed for small σ^*-values ($\bar{\alpha} > 0.1$), while for $\bar{\alpha} = 0.1$ stability appears in the total range presented here.
4. It was also found that for certain low surface tension parameters σ^*, the viscous liquid sphere ceases to oscillate, just performing an aperiodic motion. This is valid for an unrestrained liquid globule and a captured liquid drop as well. With the increase of the cap angle $\bar{\alpha}$, the critical decay magnitude shifts to larger values for each mode. This is also true for fixed mode numbers, where with the increase of the cap angle $\bar{\alpha}$, the critical decay magnitude increases, indicating for larger $\bar{\alpha}$-values and higher modes a rapid decay, if disturbed.

Acknowledgements

The authors would like to thank Mr. H. Kimura, Graduate School of Iwate University, Japan, for his help in the numerical calculations.

References

[1] J.A.F. Plateau, Experimental and theoretical researches on the figures of equilibrium of a liquid mass withdrawn from the action of gravity, Annual Report of the Broad of Regents and Smithsonian Institution, Government Printing Office, Washington, 1863, pp. 207–285; 1864, pp. 286–369; 1865, pp. 411–435; 1866, pp. 255–289.
[2] L. Rayleigh, On the capillary phenomena, *Proceedings of the Royal Society* 29 (1879) 71–97.
[3] L. Rayleigh, *The Theory of Sound*, Dover Publication, New York, 1945.
[4] H. Lamb, *Hydrodynamics*, Dover Publication, New York, 1945, pp. 451–457, 632–642.
[5] H. Lamb, On the oscillations of a viscous spheroid, *Proceedings of the London Mathematical Society* 53 (1881) 51–66.
[6] C.A. Miller, L.E. Scriven, The oscillations of a fluid droplet immersed in another fluid, *Journal of Fluid Mechanics* 32 (1968) 417–435.

[7] A. Prosperetti, Normal-mode analysis for the oscillations of a viscous liquid drop in an immiscible liquid, *Journal de Mecanique* 19 (1980) 149–182.
[8] H.F. Bauer, Oscillations of immiscible liquids in free space or in spherical containers in zero-gravity environment, *Ingenieur Archiv* 51 (1982) 363–381.
[9] H.F. Bauer, Natural frequencies and stability of immiscible spherical liquid system, *Applied Microgravity Technology* 1 (1988) 90–102.
[10] H.F. Bauer, Surface- and interface oscillations of freely floating spheres of immiscible viscous liquids, *Ingenieur Archiv* 53 (1983) 371–383.
[11] J.A. Tsamopoulos, R.A. Brown, Nonlinear oscillations of inviscid drops and bubbles, *Journal of Fluid Mechanics* 127 (1983) 519–537.
[12] H.F. Bauer, W. Eidel, Nonlinear liquid oscillations in spherical systems under zero-gravity, *Acta Mechanica* 65 (1986) 107–126.
[13] G.G. Foote, A Theoretical Investigation of the Dynamics of Liquid Drops, PhD Thesis, University of Arizona, 1971.
[14] H.F. Bauer, Oscillations of a visco-elastic liquid drop in zero-gravity, *Proceedings of the Fifth European Symposium on Material Science Under Microgravity*, Schloß Elmau, 1984 (ESA-SP-222).
[15] H.F. Bauer, Surface- and interface oscillations in an immiscible spherical visco-elastic system, *Acta Mechanica* 55 (1985) 127–149.
[16] H.F. Bauer, W. Eidel, Vibration of a visco-elastic spherical immiscible liquid system, *Zeitschrift für Angewandte Mathematik und Mechanik* 67 (1987) 525–535.
[17] H.F. Bauer, M. Chiba, Oscillations of a captured spherical drop of frictionless liquid, *Journal of Sound and Vibration* 274 (2004) 725–746.
[18] C. Bisch, A. Lasek, H. Rodot, Comportement hydrodynamique de volumes liquides sphériques semi-libres en apesanteur simulée, *Journal de Mécanique Théorique et Appliquée* 1 (1982) 165–183.